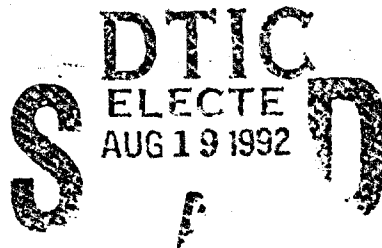JHU/APL
TG 1383
AUGUST 1992

*Technical Memorandum*

# A NEW MODEL FOR INTERPRETING EXPERIMENTAL DATA FROM A CIRCULAR WAVEGUIDE CAVITY

WILLIAM A. HUTING

**Reproduced From
Best Available Copy**

THE JOHNS HOPKINS UNIVERSITY ■ APPLIED PHYSICS LABORATORY

92 8 17 003

JHU/APL
TG 1383
AUGUST 1992

*Technical Memorandum*

# A NEW MODEL FOR INTERPRETING EXPERIMENTAL DATA FROM A CIRCULAR WAVEGUIDE CAVITY

WILLIAM A. HUTING

THE JOHNS HOPKINS UNIVERSITY ■ APPLIED PHYSICS LABORATORY
Johns Hopkins Road, Laurel, Maryland 20723-6099

SECURITY CLASSIFICATION OF THIS PAGE

# REPORT DOCUMENTATION PAGE

| 1a. REPORT SECURITY CLASSIFICATION<br>UNCLASSIFIED | 1b. RESTRICTIVE MARKINGS |
|---|---|
| 2a. SECURITY CLASSIFICATION AUTHORITY | 3. DISTRIBUTION/AVAILABILITY OF REPORT |
| 2b. DECLASSIFICATION/DOWNGRADING SCHEDULE | Approved for public release; distribution unlimited |

| 4. PERFORMING ORGANIZATION REPORT NUMBER(S)<br>JHU/APL TG-1383 | 5. MONITORING ORGANIZATION REPORT NUMBER(S)<br>JHU/APL TG-1383 |
|---|---|

| 6a. NAME OF PERFORMING ORGANIZATION<br>The Johns Hopkins University<br>Applied Physics Laboratory | 6b. OFFICE SYMBOL<br>(If applicable)<br>TIR | 7a. NAME OF MONITORING ORGANIZATION<br>The Johns Hopkins University<br>Applied Physics Laboratory |
|---|---|---|
| 6c. ADDRESS (City, State, and ZIP Code)<br>Johns Hopkins Road<br>Laurel, Md. 20723-6099 | | 7b. ADDRESS (City, State, and ZIP Code)<br>Johns Hopkins Road<br>Laurel, Md. 20723-6099 |
| 8a. NAME OF FUNDING/SPONSORING ORGANIZATION<br>Dept. of the Navy<br>Naval Sea Systems Command O6C | 8b. OFFICE SYMBOL<br>(If applicable) | 9. PROCUREMENT INSTRUMENT IDENTIFICATION NUMBER<br>N00039-91-C-0001 |

| 8c. ADDRESS (City, State, and ZIP Code)<br><br>NC-2 Crystal City, Va. 20362 | 10. SOURCE OF FUNDING NUMBERS | | | |
|---|---|---|---|---|
| | PROGRAM ELEMENT NO. | PROJECT NO. | TASK NO.<br>BKHR9LXX F2F | WORK UNIT ACCESSION NO. |

11. TITLE (Include Security Classification)

A New Model for Interpreting Experimental Data from a Circular Waveguide Cavity (U)

12. PERSONAL AUTHOR(S)

William A. Huting

| 13a. TYPE OF REPORT<br>Technical Memorandum | 13b. TIME COVERED<br>FROM _____ TO _____ | 14. DATE OF REPORT (Year, Month, Day)<br>92-8-7 | 15. PAGE COUNT<br>20 |
|---|---|---|---|

16. SUPPLEMENTARY NOTATION

| 17. | COSATI CODES | | 18. SUBJECT TERMS (Continue on reverse if necessary and identify by block number) |
|---|---|---|---|
| FIELD | GROUP | SUB-GROUP | Waveguide          Attenuation |
| | | | Resonator          Microwaves |

19. ABSTRACT (Continue on reverse if necessary and identify by block number)

Progress is described in the testing of circular $TE_{01}$ waveguide using a resonant cavity technique. A new model has been developed for extrapolating insertion loss values from experimental cavity $Q$ data. This model is compared with a previous model, and experiments are described that involve both cavities with mechanically adjustable lengths and cavities with fixed lengths. Data are also presented for waveguide bend cavities. In all cases, the extrapolated traveling wave losses were in good agreement with the theory.

| 20. DISTRIBUTION/AVAILABILITY OF ABSTRACT<br>☒ UNCLASSIFIED/UNLIMITED  ☐ SAME AS RPT.  ☐ DTIC USERS | 21. ABSTRACT SECURITY CLASSIFICATION<br>UNCLASSIFIED |
|---|---|
| 22a. NAME OF RESPONSIBLE INDIVIDUAL<br>NAVTECH REP Security Officer | 22b. TELEPHONE (Include Area Code)<br>(301) 953-5403 | 22c. OFFICE SYMBOL<br>NAVTECH REP |

DD FORM 1473, 84 MAR          83 APR edition may be used until exhausted.          SECURITY CLASSIFICATION OF THIS PAGE
All other editions are obsolete.

# ABSTRACT

Progress is described in the testing of circular $TE_{01}$ waveguide using a resonant cavity technique. A new model has been developed for extrapolating insertion loss values from experimental cavity $Q$ data. This model is compared with a previous model, and experiments are described that involve both cavities with mechanically adjustable lengths and cavities with fixed lengths. Data are also presented for waveguide bend cavities. In all cases, the extrapolated traveling wave losses were in good agreement with the theory.

DTIC QUALITY INSPECTED 8

| Accesion For | | |
|---|---|---|
| NTIS CRA&I | | ☑ |
| DTIC TAB | | ☐ |
| Unannounced | | ☐ |
| Justification | | |
| By | | |
| Distribution / | | |
| Availability Codes | | |
| Dist | Avail and/or Special | |
| A-1 | | |

# CONTENTS

# ILLUSTRATIONS

# TABLES

# 1. INTRODUCTION

Circular $TE_{01}$ waveguide is currently being investigated for low-loss use, and this paper describes progress in the testing of such waveguide using a resonant cavity technique. This technique is useful because long lengths of waveguide are not always available for testing, and the attenuation in short sections of waveguide can be too small to measure directly. An alternative is to convert a short waveguide section into a variable-length cavity by attaching a metal plate to one end and inserting a conducting piston into the other end as shown in Figure 1. $Q$ data (the $Q$, or Quality Factor, of a cavity is the resonant frequency divided by the 3-dB bandwidth of the cavity excitation response) are then obtained at several resonant lengths for a fixed center frequency.[1] The next step is to compute a numerical value for the traveling wave insertion loss from these $Q$ data.

In this paper, a new relation is derived for extrapolating an insertion loss figure from the cavity $Q$ figures, and this new model is compared with an older one published by Karbowiak and Skedd.[1] Test results are also presented. The new model can also be modified for use in determining the insertion loss of nonuniform waveguide sections. For example, a 90° circular–cross-section waveguide bend has been tested at 3.3 GHz. $Q$ data indicate a loss that is in good agreement with previous theory. Finally, the potential applicability of the new model to the problem of using fixed-length cavities to determine waveguide attenuation is described.

The waveguide sections tested were made of sheathed-helix waveguide (see Fig. 2). This waveguide consists of a tightly wound insulated wire surrounded by a lossy dielectric, which is in turn encapsulated by a good conductor. The purpose of this
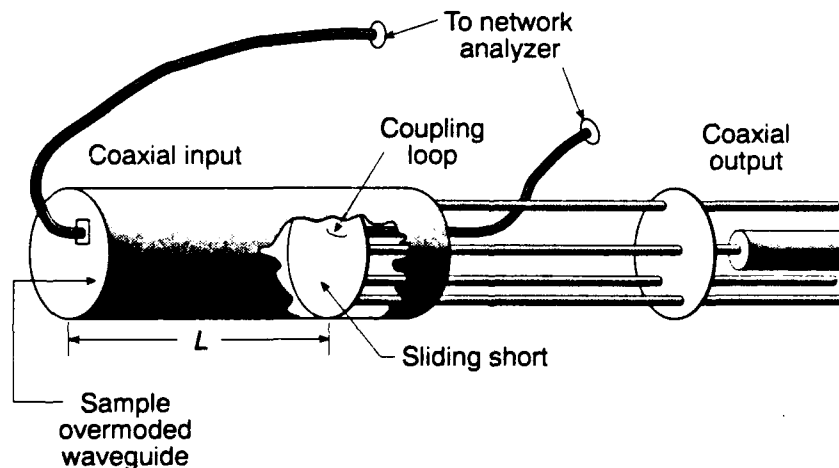


**Figure 1** Variable-length cavity test configuration.

[1] A. E. Karbowiak, and R. F. Skedd, "Testing of Circular Waveguides Using a Resonant Cavity Method," *Proc. IEE* **106B**. Supplement 13, 66–70 (Sep 1959).
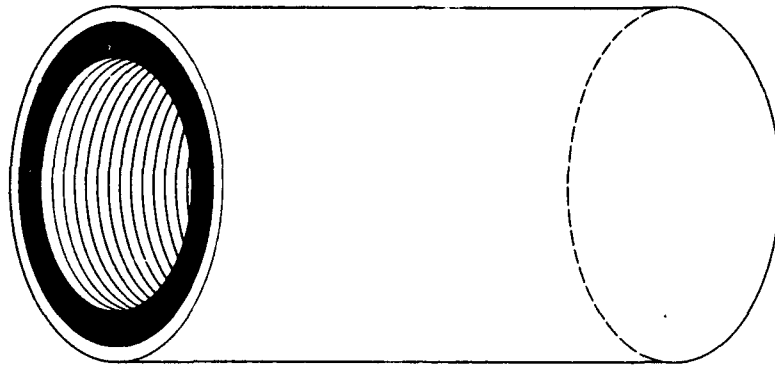
**Figure 2**  Sheathed-helix waveguide.

configuration is to suppress all the modes except the $TE_{01}$ mode. Various design and development issues are described in Reference 2. Methods for establishing theoretical insertion losses for these devices are also given in Reference 2.

# 2.  VARIABLE–LENGTH STRAIGHT CAVITIES

In this paper, tests are described that quantify insertion loss for circular overmoded waveguide. The two basic test configurations are shown in Figures 1 and 3. Figure 3 depicts a traveling wave test configuration, which is made possible by using a rectangular $TE_{10}$ to circular $TE_{01}$ mode transducing waveguide section. The transition used in these tests was the Marie transducer,[3] a device discussed at some length in References 4 and 5. Unfortunately, precise determination of insertion losses for relatively short sections of waveguide using this setup is not practical because the predicted low losses are beyond the sensitivity of the measurement apparatus. This configuration is very useful, however, in investigating bends, as will be discussed later in this paper. All the experimental data presented herein were obtained using an automatic network analyzer.

Tests using the configuration presented in Figure 1 will now be described. Initially, the endplates were of the type depicted in Figure 4 with a coupling half-loop located

[2]W. A. Huting, J. W. Warren, and J. A. Krill, "Recent Progress in Circular High-Power Overmoded Waveguide," *Johns Hopkins APL Tech. Dig.* **12**(1), 60–74 (1991).

[3]G. R. P. Marie, *Mode Transforming Waveguide Transition*, U. S. Patent No. 2,859,412, 4 Nov 1958.

[4]S. S. Saad, J. B. Davies, and O. J. Davies, "Analysis and Design of a Circular $TE_{01}$ Mode Transducer," *IEE J. Microwaves Opt. Acoust.* **1**, 58–62 (Jan 1977).

[5]S. S. Saad, J. B. Davies, and O. J. Davies, "Computer Analysis of Gradually Tapered Waveguide with Arbitrary Cross Sections," *IEEE Trans. on Microwaves Theory Tech.* **MTT-25**, 437–440 (May 1977).
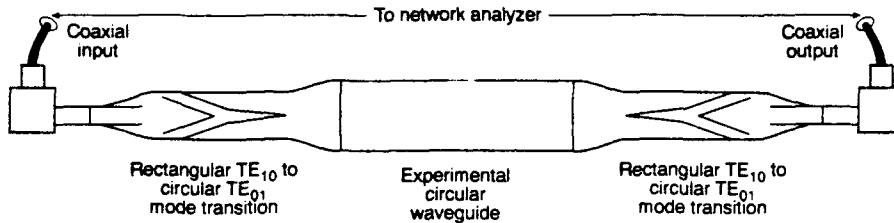
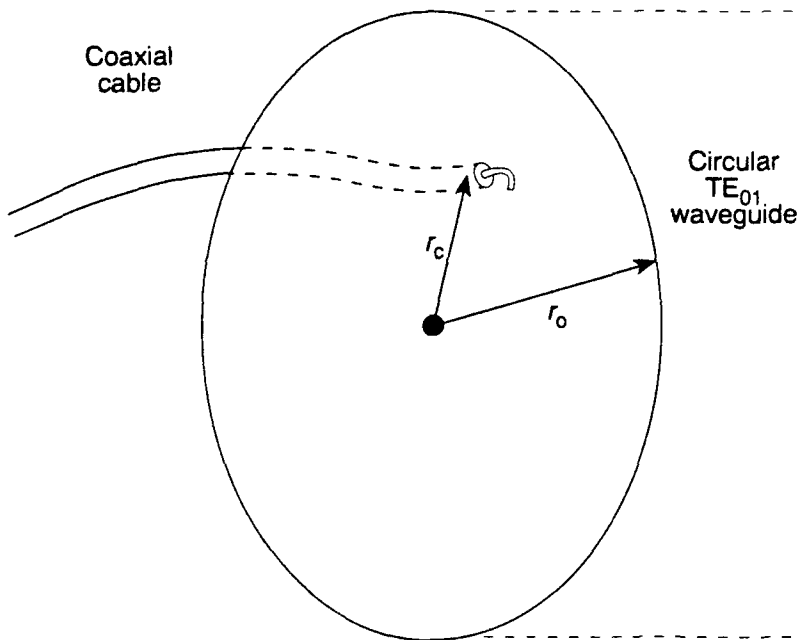**Figure 3** Traveling wave test configuration.



**Figure 4** Endplate used in variable-length cavity tests. The plane of the coupling loop was perpendicular to the radius vector, and $r_c = 0.4804\ r_o$.

slightly off-center between the cavity axis and the helix to maximize $TE_{01}$ coupling. As a first step in constructing a theoretical model for this cavity, one may define a $2 \times 2$ scattering matrix describing the cavity endplates, which are assumed to be identical. The subscript "1" refers to the TEM mode of the coaxial line, and the subscript "2" refers to the $TE_{01}$ mode of the circular waveguide as shown in Figure 5. The scattering parameters of this system are denoted $S_{11}$, $S_{12}$, $S_{21}$, and $S_{22}$. A simple cascading formulation (see Ref. 6) may be used to determine the transmission coefficient $T$ of the entire system (i.e., Fig. 6):

[6]R. H. Dicke, "General Microwave Theorems," in *Principles of Microwave Circuits*, C. G. Montgomery, R. H. Dicke, and E. M. Purcell (eds.), McGraw-Hill, New York, pp. 130–161 (1948).

$$T = \frac{S_{12}^2}{-S_{22}^2 \exp(-\alpha_{01}L)\exp(-j\beta_{01}L) + \exp(\alpha_{01}L)\exp(j\beta_{01}L)}, \qquad (1)$$

where $\alpha_{01}$ is the $TE_{01}$ attenuation, $\beta_{01}$ is the $TE_{01}$ wave number, and $L$ is the cavity length. Let $\omega_0$ be the resonant frequency of a perfectly conducting cavity. Computing the magnitude of $T$ and expanding $\exp(\pm j\beta_{01}L)$ in a Taylor series about $\omega = \omega_0$, one obtains an expression in this form:

$$|T|^2 = \frac{K}{(\omega - \omega_0 - \delta\omega)^2 + \left(\dfrac{\omega_0 + \delta\omega}{2Q}\right)^2}. \qquad (2)$$

Here, the transmission coefficient $T$ has a 3-dB bandwidth equal to $(\omega_0 + \delta\omega)/Q$, $K$ is a parameter independent of frequency, and $\delta\omega$ is the (extremely small) shift of the resonant frequency due to losses. Expressions in the form of Equation 2 are discussed in many textbooks (e.g., Ref. 7, p. 357). The previously mentioned expansion of $exp\,(\pm j\beta_{01}L)$ also yields the following relations:

$$\delta\omega = \frac{S_{22r}S_{22i}\omega_0\beta_{01}^2(\omega_0)}{\left\{\left(S_{22r}^2 - S_{22i}^2\right)\omega_0^2\mu_0\epsilon_0 L[\beta_{01}(\omega_0)] - S_{22r}S_{22i}\left[(\beta_{01}(\omega_0))^2 - \omega_0^2\mu_0\epsilon_0\right]\right\}} \qquad (3)$$

and

$$\left(\frac{\omega_0 + \delta\omega}{2Q}\right)^2 + (\delta\omega)^2 = \qquad (4)$$

$$\frac{\left(S_{22r}^2 + S_{22i}^2\right)^2 \exp(-2\alpha_{01}L) + \exp(2\alpha_{01}L) - 2\left(S_{22r}^2 - S_{22i}^2\right)}{\left\{4\left(S_{22r}^2 - S_{22i}^2\right)L^2\omega_0^2\mu_0^2\epsilon_0^2 / [\beta_{01}(\omega_0)]^2\right.}$$

$$\left. - 4 \times S_{22r}S_{22i}L\left[\frac{\mu_0\epsilon_0}{\beta_{01}(\omega_0)} - \frac{\omega_0^2\mu_0^2\epsilon_0^2}{[\beta_{01}(\omega_0)]^3}\right]\right\}.$$

In Equations 3 and 4, the variables $S_{mnr}$ and $S_{mni}$ denote, respectively, the real and imaginary parts of the endplate scattering parameters, $\epsilon_0$ is the free-space permittivity, and $\mu_0$ is the free-space permeability. Equations 3 and 4 provide the relations for extracting values for $\alpha_{01}$ from the experimental data. For example, when a 2-ft-long, 16-cm-inner-diameter section of S-band helical waveguide was investigated, $Q$'s were obtained at $(\omega_0 + \delta\omega)/2\pi = 3.3$ GHz for nine resonant lengths. These data, when substituted into Equations 3 and 4, resulted in nine equations (corresponding to the nine measurements) in three unknowns: $S_{22r}$, $S_{22i}$, and $\alpha_{01}$. Values for these parameters were established using a least-mean-squares approach, and, for five different cavities, the computed values for $\alpha_{01}$ were between 3% below and 74% above the theoretical value (0.00299 dB/m). As an alternative to this computationally intensive procedure,

---

[7] J. D. Jackson, *Classical Electrodynamics*, 2nd Ed., Wiley, New York (1975).
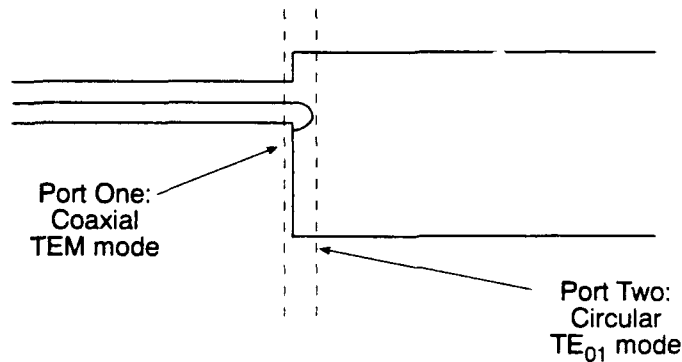
**Figure 5** Reference ports for the scattering matrix $\begin{pmatrix} S_{11} & S_{12} \\ S_{21} & S_{22} \end{pmatrix}$.
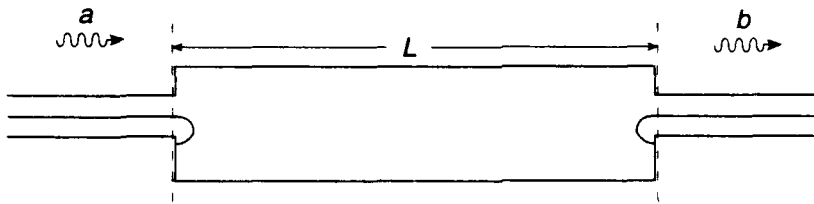


**Figure 6** Generalized cavity geometry. Let *a* and *b* denote the forward-traveling TEM wave amplitudes at the input and output ends of the cavity. The transmission coefficient *T* is defined by *b* = *Ta*.

one might want to use the following simple linear relation originally given by Karbowiak and Skedd in Reference 1:

$$\Delta f = \frac{\lambda_o^2}{\pi \lambda_g} f_o \left( \alpha_{01} + \frac{C}{L} \right), \tag{5}$$

where

$\Delta f$ = 3-dB bandwidth,

$\lambda_o$ = free-space wavelength,

$\lambda_g$ = guide wavelength,

$f_o$ = resonant frequency,

$C$ = a parameter independent of cavity length that is determined by the endplate properties, and

$L$ = cavity length.

When a linear fit was applied to the nine points ($\Delta f$, $1/L$), the extrapolated values of $\alpha_{01}$ for the five different cavities were between 37% above and 75% above the theoretical attenuation. Figure 7 shows both experimental and numerical ($\Delta f$, $1/L$) data for one of the cavities. The numerical data were generated using these least-mean-square values: $\alpha_{01}$ = 0.00290 dB/m, $S_{22r}$ = −0.9988, and $S_{22i}$ = 0.0136. The linear characteristic predicted by Karbowiak and Skedd is also predicted by the new model;
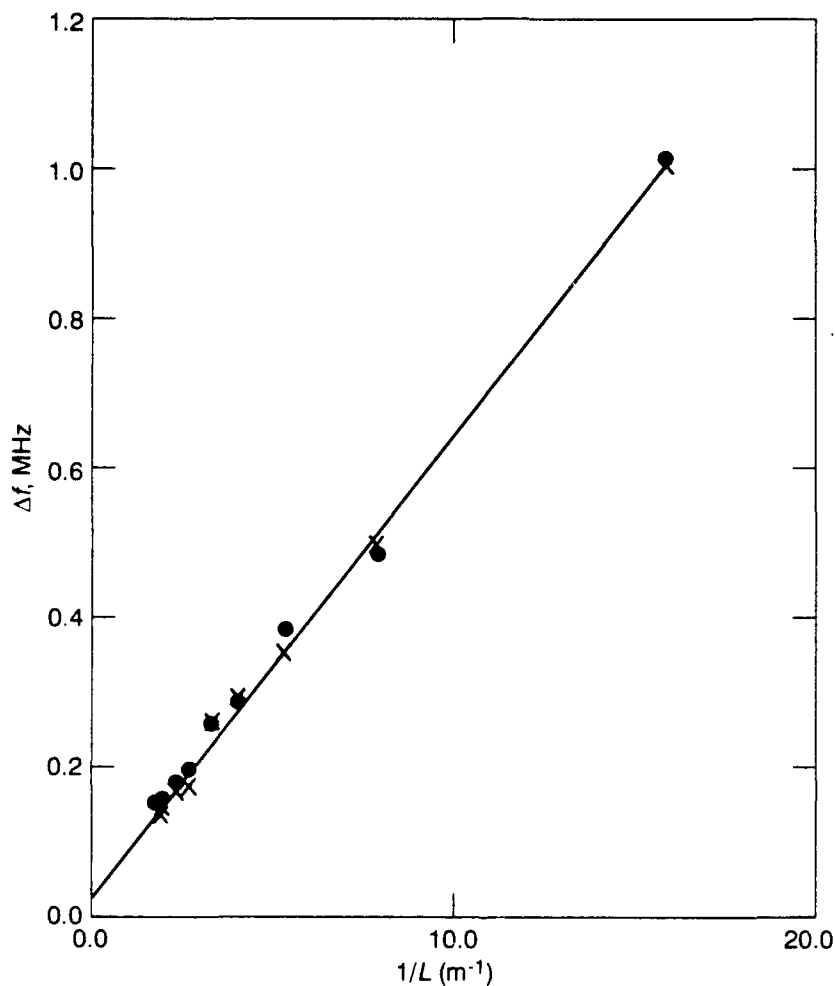
**Figure 7** Experimental (x) and numerical (·) data for a 2-ft-long, 16-cm-inner-diameter sheathed-helix waveguide cavity at 3.3 GHz. The solid line is a linear fit of the experimental data. For this short cavity, Karbowiak's model and the new model are in good agreement.

moreover, the extrapolated $\alpha_{01}$ values are nearly the same in either model. Additionally, an 8-ft-long straight waveguide section has been investigated at 3.3 GHz. Performing a linear fit on the experimental data results in a line with a negative slope as shown in Figure 8; the extrapolated attenuation value is about ten times the theoretical value. Use of the new model, however, results in an attenuation of 0.00389 dB/m. Thus, the new model appears to be useful for both long and short cavities; the model of Karbowiak and Skedd appears to be useful only for short cavities.

Sources of possible measurement error will now be described. According to the network analyzer operating manual, transmission ($|T|^2$) measurements were accurate to within ±0.1 dB.[8] Substitution of these bounds into Equation 2 results in additional

---

[8] *Model 360 Vector Network Analyzer Operation Manual*, Revision C, Wiltron Company, Morgan Hill, Ca., p. 1-9 (1987).
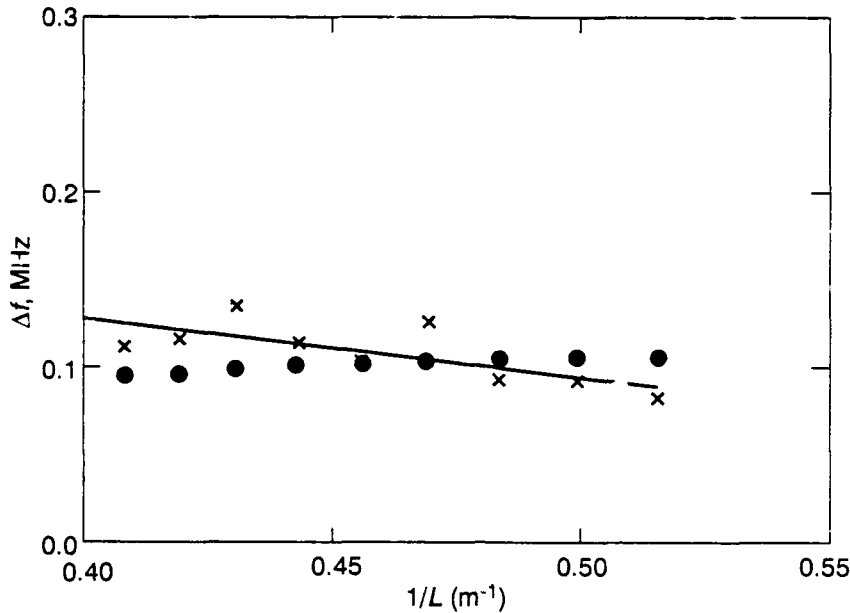
**Figure 8** Experimental (x) and numerical (·) data for an 8-ft-long, 16-cm-inner-diameter sheathed-helix waveguide cavity at 3.3 GHz. The solid line is a linear fit of the experimental data. For this long cavity, the new model is in good agreement with theory but in poor agreement with Karbowiak's model.

bounds on the accuracy of the measured $Q$'s and 3-dB bandwidths. One then allows the 3-dB bandwidth in Equation 5 to vary within these computed bounds in order to predict a range for the extrapolated insertion losses. When this was done for the S-band waveguide, the ratio between the highest and lowest extrapolated attenuations was approximately 1.5. This range is consistent with our data.

## 3. BEND CAVITIES

The methods described above may be modified to determine the transmission properties of a waveguide bend. One such bend, made out of circular sheathed-helix waveguide, is shown in Figure 9. The $TE_{01}$ transmission coefficient of the bend will be denoted $\exp(-M/8.68)\exp(-j\Delta)$; $M$ is the insertion loss in dB. The investigations of the bend were slightly complicated by the inability to push the straight piston in very far. Several ways of circumventing this difficulty exist. For example, one could begin by measuring the phase shift $\Delta$ of the bend to facilitate the far more important task of determining insertion loss. The phase shift and its derivative $d\Delta/d\omega$ may be obtained using the traveling wave setup of Figure 3. (The two Marie transducers must be measured directly connected to one another, and their combined phase shift is
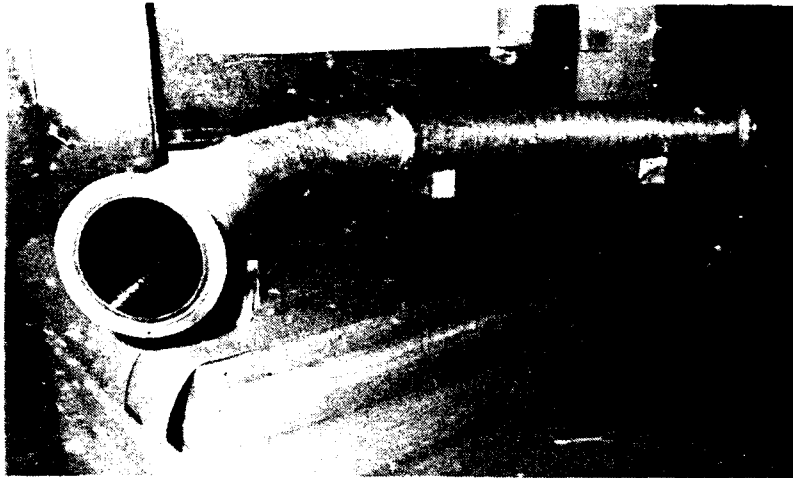
**Figure 9**  S-band sheathed-helix waveguide bend.

subtracted from that of the entire system to yield $\Delta$.) Then a cavity is made by connecting endplates to the bend. The transmission coefficient of the cavity is of the form of Equation 1 with $M/8.68$ replacing $\alpha_{01}L$ and $\Delta$ replacing $\beta_{01}L$. Relations similar to Equations 3 and 4 may be derived from this cavity transmission coefficient. Determination of the bend insertion loss is expedited by comparing the $Q$ of a bend cavity with that of a straight cavity. If one experimentally verifies that $d(\beta_{01}L)/d\omega = d\Delta/d\omega$ (as described above), then the following relation applies:

$$\left(\frac{Q_{\text{bend}}}{Q_{\text{straight}}}\right)^2 = \tag{6}$$

$$\frac{\left(S_{22r}^2 + S_{22i}^2\right)^2 \exp(-2\alpha_{01}L) + \exp(2\alpha_{01}L) - 2\left(S_{22r}^2 - S_{22i}^2\right)}{\left(S_{22r}^2 + S_{22i}^2\right)^2 \exp(-M/8.68) + \exp(M/8.68) - 2\left(S_{22r}^2 - S_{22i}^2\right)}$$

Equation 6 was derived by neglecting $(\delta\omega)^2$ and finding the ratio of Equation 4 to the corresponding expression for a bend cavity. Making the approximations $S_{22r} = -1$, $S_{22i} = 0$, and using a series expansion of the exponential terms, Equation 6 reduces to the following:

$$M = 8.68\alpha_{01}L(Q_{\text{straight}} / Q_{\text{bend}}). \tag{7}$$

In Equation 7, $M$ is in dB, and $\alpha_{01}$ is in Np/m. If the straight waveguide attenuation $\alpha_{01}$ is known, then Equation 7 may be used to determine the bend insertion loss $M$. In Section 2, $Q$ measurements were used to establish lower and upper bounds on $\alpha_{01}$ for S-band sheathed-helix waveguide. The $Q$'s of an S-band bend and a 7.32-ft S-band straight cavity have also been measured near 3.3 GHz (see Table 1). The extrapolated insertion loss value for the bend was in the range $0.027 \text{ dB} \leq M \leq 0.049$ dB. The theoretical loss (see Ref. 2, Eq. 1) is $M = 0.025$ dB. The actual bend loss may, in fact, be higher than this theoretical figure because the theory does not take into account the unavoidable exposure of the sheath caused by different portions of the wire separating from each other in the outer radius of a waveguide bend.

**Table 1**

Measured $Q$'s for an S-band bend and a 7.32-ft S-band straight cavity. The movable conducting piston was adjusted so that both cavities were 7.32-ft long.

| Frequency (MHz) | $Q$, Straight* | $Q$, Bend** |
|---|---|---|
| 3283 | 24970 | 6950 |
| 3332 | 23070 | 6810 |

*Average $Q$ = 24020. **Average $Q$ = 6880.

## 4. FIXED–LENGTH STRAIGHT CAVITIES

In this section, the new model is used to extrapolate insertion loss values from the $Q$ data of a fixed-length cavity. This approach differs from the previously described techniques principally in that $S_{22r}$ and $S_{22i}$ must be known before the measurements.
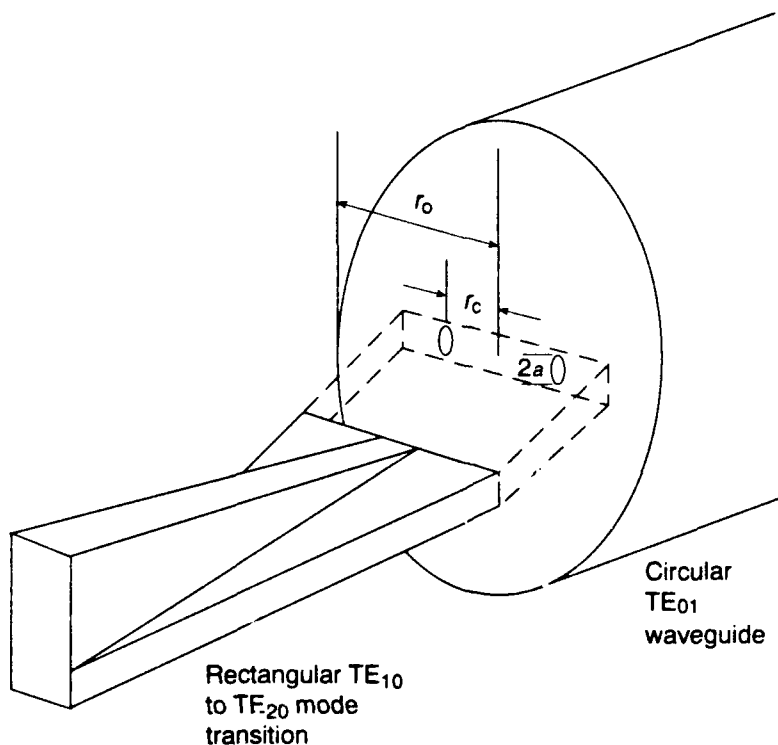


**Figure 10**   Endplate assembly used in fixed-length cavity tests. The aperture diameter $2a$ was equal to 0.635 cm, and $r_c$ = 0.4804 $r_o$.

For these tests, the pair of coupling apertures shown in Figure 10 were used; the subscript "1" now refers to the rectangular $TE_{20}$ mode. Using a quasistatic model, the following expression for $S_{22}$ may be derived from Equation 61b on page 503 of Reference 9:

$$S_{22} = -1 + j\omega\gamma\mu_o \mathbf{H}_n^+ \cdot \mathbf{M}.$$ (8)

Here, $\mathbf{M}$ is the magnetic dipole moment of the aperture (see Eqs. 69b and 72, pp. 507 and 508, of Ref. 9) and $\mathbf{H}_n^+$ is the magnetic field (suitably normalized) of the $TE_{01}$ mode (Ref. 9, p. 359). The parameter $\gamma$ is set equal to unity for conventional Bethe theory (e.g., Ref. 9); however, a model proposed by Collin (Ref. 9, pp. 508–511) may be used with the following result:

$$\gamma = \left(1 - j\frac{2}{9\pi}k_o^3 a^3\right)^{-1},$$ (9)

where $a$ is the aperture radius as shown in Figure 10. When Equation 9 is substituted into Equation 8, numerical verification that $|S_{22}|^2 < 1$ is possible. This condition is not met by the Bethe model. In any case, one may substitute these theoretical values for $S_{22r}$ and $S_{22i}$ into Equation 4; the additional substitution of a measured $Q$ results in a quadratic equation in $\exp(-2\alpha_{01}L)$. A 4-ft-long, 12-cm-inner-diameter sheathed-helix waveguide cavity was observed to have a $Q$ of 58477.0 at 4.42 GHz. Using Equation 9, the extrapolated value for $\alpha_{01}$ was 0.01085 dB/m as compared with a theoretical value of 0.0004762 dB/m. Improvement in the agreement between these two values could perhaps be achieved through the development of a better model for the aperture. The development of such an aperture model is being pursued.

# 5. CONCLUSIONS

A new model for interpreting data from a circular cylindrical cavity has been developed. This model is applicable to both fixed- and variable-length waveguide cavities. It is applicable to nonuniform cavities as long as the two endplates are of identical design. Experimental data have been presented, and the insertion loss values extrapolated from these data are in good agreement with the values predicted from the theory.

9R. E. Collin, *Field Theory of Guided Waves*, 2nd Ed., IEEE Press, New York (1991).

# REFERENCES

[1] A. E. Karbowiak, and R. F. Skedd, "Testing of Circular Waveguides Using a Resonant Cavity Method," *Proc. IEE* **106B**, Supplement 13, 66–70 (Sep 1959).

[2] W. A. Huting, J. W. Warren, and J. A. Krill, "Recent Progress in Circular High-Power Overmoded Waveguide," *Johns Hopkins APL Tech. Dig.* **12**(1), 60–74 (1991).

[3] G. R. P. Marie, *Mode Transforming Waveguide Transition*, U. S. Patent No. 2,859,412, 4 Nov 1958.

[4] S. S. Saad, J. B. Davies, and O. J. Davies, "Analysis and Design of a Circular $TE_{01}$ Mode Transducer," *IEE J. Microwaves Opt. Acoust.* **1**, 58–62 (Jan 1977).

[5] S. S. Saad, J. B. Davies, and O. J. Davies, "Computer Analysis of Gradually Tapered Waveguide with Arbitrary Cross Sections," *IEEE Trans. on Microwaves Theory Tech.* **MTT-25**, 437–440 (May 1977).

[6] R. H. Dicke, "General Microwave Theorems," in *Principles of Microwave Circuits*, C. G. Montgomery, R. H. Dicke, and E. M. Purcell (eds.), McGraw-Hill, New York, pp. 130–161 (1948).

[7] J. D. Jackson, *Classical Electrodynamics*, 2nd Ed., Wiley, New York (1975).

[8] *Model 360 Vector Network Analyzer Operation Manual*, Revision C, Wiltron Company, Morgan Hill, Ca., p. 1-9 (1987).

[9] R. E. Collin, *Field Theory of Guided Waves*, 2nd Ed., IEEE Press, New York (1991).

# INITIAL DISTRIBUTION EXTERNAL TO THE APPLIED PHYSICS LABORATORY*

| ORGANIZATION | LOCATION | ATTENTION | No. of Copies |
|---|---|---|---|
| **DEPARTMENT OF DEFENSE** | | | |
| Defense Technical Information Center | Alexandria, VA 23314 | Accessions | 12 |
| **DEPARTMENT OF THE NAVY** | | | |
| Naval Air Systems Command | Washington, DC 22202 | Library, Air 7226 | 2 |
| Naval Sea Systems Command O6C | NC-2 Crystal City, VA 20362 | M. J. O'Driscoll | 1 |
| Naval Surface Warfare Center–Crane Division | Crane, IN 47522 | G. Kreager | 2 |
| NAV TECH REP | Laurel, MD 20723-6099 | | 2 |
| SPAWAR | Arlington, VA 20363-5100 | Library | 2 |
| **OTHERS** | | | |
| Purdue University | West Lafayette, IN 47907 | K. J. Webb | 1 |

**Requests for copies of this report from DoD activities and contractors should be directed to DTIC.
Cameron Station, Alexandria, Virginia 22314 using DTIC Form 1 and, if necessary, DTIC Form 55.**

*Initial distribution of this document within the Applied Physics Laboratory has been made in accordance with a list on file in the APL Technical Publications Group.